Own-species bias in the representations of monkey and human face categories in the primate temporal lobe

R. Sigala,[1] N. K. Logothetis,[1,2] and G. Rainer[1,3]

[1]*Max Planck Institute for Biological Cybernetics, Tübingen, Germany;* [2]*Division of Imaging Science and Biomedical Engineering, University of Manchester, Manchester, United Kingdom; and* [3]*Department of Medicine, University of Fribourg, Fribourg, Switzerland*

Sigala R, Logothetis NK, Rainer G. Own-species bias in the representations of monkey and human face categories in the primate temporal lobe. *J Neurophysiol* 105: 2740–2752, 2011. First published March 23, 2011; doi:10.1152/jn.00882.2010.—Face categorization is fundamental for social interactions of primates and is crucial for determining conspecific groups and mate choice. Current evidence suggests that faces are processed by a set of well-defined brain areas. What is the fine structure of this representation, and how is it affected by visual experience? Here, we investigated the neural representations of human and monkey face categories using realistic three-dimensional morphed faces that spanned the continuum between the two species. We found an "own-species" bias in the categorical representation of human and monkey faces in the monkey inferior temporal cortex at the level of single neurons as well as in the population response analyzed using a pattern classifier. For monkey and human subjects, we also found consistent psychophysical evidence indicative of an own-species bias in face perception. For both behavioural and neural data, the species boundary was shifted away from the center of the morph continuum, for each species toward their own face category. This shift may reflect visual expertise for members of one's own species and be a signature of greater brain resources assigned to the processing of privileged categories. Such boundary shifts may thus serve as sensitive and robust indicators of encoding strength for categories of interest.

macaque; electrophysiology; perception; psychophysics

THE ABILITY to rapidly sort stimuli into categories is central to cognition in primates, and its neural basis continues to be a major focus of experimental studies in cognitive neuroscience. In monkeys, neural activity has been shown to correlate with categorical judgements (Akrami et al. 2009; Baker et al. 2002; Freedman and Assad 2006; Freedman et al. 2003; Sigala and Logothetis 2002). This work clearly shows that behavioral training strongly influences neural responses to stimulus categories, emphasizing that learned contingencies in particular tasks are reflected in higher-level visual cortexes. A separate line of investigation has focused on the representation of natural categories in the inferior temporal (IT) cortex (Kiani et al. 2007; Kriegeskorte et al. 2008; Quiroga et al. 2005; Vogels 1999) by investigating visual responses to large sets of stimuli from natural categories. These studies focused on studying the structure of the representation of stimulus categories that observers have acquired during their everyday experience with these stimuli. It has been shown that neural response patterns tend to form clusters that correspond to natural categories (Kiani et al. 2007). The representation of natural categories has also been extensively investigated using functional neuroimaging. These studies have focused on delineating regions of cortex that are metabolically active during the processing of particular stimulus categories (Grill-Spector et al. 2004; Haxby et al. 2001; Tsao et al. 2006). Of particular interest is a recent study (Kriegeskorte et al. 2008) that compared the representation of natural object categories in the IT cortex of humans and macaque monkeys. The category representations indeed share many characteristics in the two species, suggesting that a common code may exist in the primate temporal lobe for natural categories. This notion is also supported by another recent functional neuroimaging study (Tsao et al. 2008) that suggested an anatomic correspondence between face-selective areas defined in human and monkey brains. The existence of such a common code suggests that categorization of natural stimulus categories might not be as flexible as the work using behavioral paradigms suggests but conforms with a rather fixed structure that is conserved across primate species. Nevertheless, specific visual experiences of humans and monkeys might cause systematic variations in the natural category representation in each species. To address how experience shapes categorical representations, we focused on the representation of own- and other-species faces, natural categories for which we expected that differences in perception and neural representation might exist between monkey and human observers. We used realistic three-dimensional (3-D) morphed faces that spanned the continuum between humans and monkeys. Responses to such morphed stimuli are critical for establishing boundaries between categorical representations (Harnad 1987). We examined the modulation of single neuron activity across the species continuum, first by verifying its existence and then determining the location of the species boundary from the neural population activity using a pattern classifier. We also used the activity of "face cells" to provide additional verification of the existence and location of the species boundary, and we present psychophysical evidence from monkey and human observers regarding the location of the species boundary.

Address for reprint requests and other correspondence: G. Rainer, Max Planck Institute for Biological Cybernetics, Spemannstrasse 38, Tübingen D-72076 , Germany (e-mail: gregor.rainer@unifr.ch).

MATERIALS AND METHODS

Stimuli. To create the human/monkey morphs, we first scanned faces of humans and monkeys using a commercial system (3DMD) to acquire 3-D information about their form and texture. We then applied a method based on Support Vector Machines (SVM) (Steinke et al. 2005) that linearly interpolates between two 3-D objects. This method can be generally divided in two algorithms. By solving an optimization problem, the first algorithm finds a representation of any 3-D object in terms of a hyperplane in Hilbert space H, given a cloud of

surface points on the face as training data. These points are obtained by scanning the real faces. After the first algorithm has created such a representation of the 3-D faces (implicitly represented by kernel machines), the second algorithm computes a dense correspondence between two surfaces (in our case, the faces) by matching them using additional feature points ("markers"). Once faces shared the same representation and were in total correspondence, we interpolated them and rendered the images using commercial software (3D Studio Max). Object stimuli were constructed from 3-D models of fruits, furniture, toys, and a human hand. All stimuli were shown in grayscale, were presented in trial-randomized views (−20 to +20°) and sizes (8–12°), and were normalized in terms of contrast and mean luminance, minimizing the influence of low-level cues. Some examples of the images used in our experiments are shown in the Supplemental Material (Supplemental Fig. S1).[1]

Monkey fixation task and recording methods. Two adult male monkeys (*Macaca mulatta*; *monkeys M1* and *M2*) participated in the experiments. All experiments were approved by the local authorities (Regierungspraesidium, Tuebingen, Germany) and followed the guidelines of the European Community (European Union directive 86/609/EEC) for the care and use of laboratory animals. Stimuli were shown on a 21-in. gamma-corrected monitor located 97 cm from the monkeys. After fixation to a spot of light presented at the center of gaze for 400 ms, a single stimulus (object or face) was presented for 500 ms in pseudorandom order. Monkeys were fixating to the single stimulus throughout each trial in a window of 1° radius. Scleral search coil sampling at 200 Hz (CNC Engineering, Enfield, CT) was used to monitor eye movements. Monkeys were rewarded with juice if they fixated through the whole trial. Recordings were done using platinum/tungsten electrodes coated with quartz glass with an impedance between 1 and 2 MΩ (ESI2ec, Thomas Recording, Giessen, Germany). Electrodes were controlled with a five-channel electrode drive (Thomas Recording). We used a chamber consisting of a ball-and-socket joint with an 18-gauge stainless steel tube passing through its center. Chambers were implanted using the following Horsley-Clark coordinates: 6 mm anterior-posterior (AP) and 25 mm mediolateral (ML) in *monkey M1* and 6 mm AP and 23.4 mm ML in *monkey M2*.

Data analysis. We recorded neural signals bandpass filtered between 100 Hz and 4 kHz. Single units were extracted using a commercial offline spike-sorting system (Offline Sorter, Plexon, Dallas, TX). Neural responses were estimated by averaging activity from 100 to 300 ms after the stimulus onset. This time window is consistent with a previous study (Sugase et al. 1999) showing that a large amount of information about face features is encoded between 100 and 200 ms after stimulus presentation. Neurons with significantly greater responses to any of the presented stimuli compared with baseline (0–200 ms before stimulus presentation) were considered as "visually responsive." To characterize the tuning properties of single neurons, we used regressors as templates, as represented by the following functions: [1 1 1 0 0 0] for "step like," [0 0.2 0.4 0.6 0.8 1] for "monotonic like," and [0 0.5 1 1 0.5 0] for "inverted U shaped." For each neuron, we constructed a vector by concatenating the mean responses to each morph trajectory (the vector length was 24 given the 4 trajectories and 6 levels/trajectory). To calculate the correlations, we concatenated four times each regressor's function to obtain vectors of the same length. Only neurons with significant correlation coefficients were labeled as one of the three classes (P value of the Pearson's correlation $< 0.05/3$, Bonferroni corrected). If a neuron significantly correlated with more than one function, its label was then assigned on the basis of the maximum absolute value of the correlation.

Neural population classifier. Population activity was represented as a matrix with 238 rows (34 unique stimuli × 7 repetitions) and as many columns as recorded neurons in each monkey. We reduced the dimensionality of the data using principal component analysis and retained 10% of the components accounting for the greatest variance in the raw data (*monkey M1*: 19 principal components, 36% of overall variance; *monkey M2*: 21 principle components, 36% of overall variance) for submission to a two-class linear SVM classifier. We used SPIDER, a Matlab toolbox that implements a SVM classifier (http://www.kyb.tuebingen.mpg.de/bs/people/spider/). For simplicity, we used a linear kernel function to estimate the dividing hyperplane, which separates the data points into two groups. However, we also tested a Gaussian (nonlinear) kernel, which showed no significant difference in the results. In all our simulations, the parameter C, which controls for the generalization error, was fixed to $C = 1$. This value was selected (using cross-validation) after assessing the performance in a subset of our data. The classifier was first used to label the neural activity elicited by ambiguous faces (morphs) as "human" or "monkey" given the pattern of activation evoked by prototypical human and monkey faces (referred to here as the "classification task"). To this effect, we trained the classifier to distinguish between the activation elicited by human and monkey faces. Training examples were 75% of the trials (randomly selected) in which prototypical faces were shown (32 of 42 trials for each category, humans and monkeys). We tested the classifier's performance on the remaining 25% of the trials corresponding to prototypical faces (10 of 42 trials/category) and all trials of the remaining morphed faces (112 trials resulting from 7 presentations of 4 faces of each morph level: 20%, 40%, 60%, and 80%). To calculate the position of the boundary, we fitted psychometric functions to the classifier's decisions using the psignifit toolbox (version 2.5.6) for Matlab (Wichmann and Hill 2001). To compute confidence intervals, we calculated the boundary using only 75% of the recorded cells (randomly selected) and repeated this procedure 100 times. Significance was tested with a nonparametric test (Wilcoxon signed-rank test) comparing the distribution of categorical boundaries against a "null hypothesis" distribution. This distribution was computed by "shuffling" the category (or labels) of the trials during training, repeating the fitting procedure, and iterating again 100 times (shuffling the labels of the training examples before iterating is a standard procedure used to compute the "baseline" performance of a classifier; we will refer to it here as "shuffled bootstraps"). The mean boundary in shuffled bootstraps was place at the center of the continuum ±2%. We also used the classifier to analyze the sensitivity of the neural population to detect differences between morph faces differing by 20% in the species continuum (referred to here as the "discrimination task"). For this, we trained the classifier with 75% of the trials (randomly selected) of each of the two morph levels contrasted (0% vs. 20%, 20% vs. 40%, 40% vs. 60%, etc., resulting in 21 of 28 trials for each morph level). Afterward, the classifier was tested with the remaining trials (7 of 28 trials for each morph level). Performance of the discrimination task (d') was computed as follows: $d' = z(\mathrm{H}) - z(\mathrm{F})$, where H is the number of "hits" or correct classifier decision and F is the number of "false alarms" or wrong classifier decisions. Both values were z-transformed to obtain d'. As in the classification task, confidence intervals were obtained using bootstrapping, and significance was tested by comparing performance against performance on shuffled bootstraps.

Transmission of category information by face cells. To select face cells, we considered a criterion based on the very first studies that systematically investigated neural responses to faces and other complex objects (Perrett 1994; Perrett et al. 1982; Perrett 1979). Accordingly, we considered as face cells neurons whose mean response to faces was greater than twice the mean response to objects (20 neurons in *monkey M1* and 9 neurons in *monkey M2*). From this population, only a few neurons significantly correlated with the three regressors defined above (step like: 3 of 20 neurons in *monkey M1* and 0 of 9 neurons in *monkey M2*, monotonic like: 5 of 20 neurons in *monkey M1* and 1 of 9 neurons in *monkey M2*, and inverted U shaped: 4 of 20 neurons in *monkey M1* and 1 of 9 neurons in *monkey M2*). For each face cell, we computed the mutual information between responses to pairs of face stimuli adjacent in the morph continuum (0% vs. 20%,

[1] Supplemental Material for this article is available at the *Journal of Neurophysiology* website.

20% vs. 40%, 40% vs. 60%, etc.). The mutual information I(S,R) quantifies how well different neural responses (R) discriminate between different stimuli (S). Here, we were interested in how the responses of a neuron discriminated between two adjacent morph levels. I(S,R) was estimated in the following form:

$$I(S|R) = \sum_{r,s} P(s)P(r|s)\log_2\frac{P(r|s)}{P(r)}$$

where P is the probability. Intuitively, I(S,R) quantifies the reduction of uncertainty (entropy) about the stimulus gained after observing the response to this stimulus. For each trial, we counted the number of spikes within 100 and 300 ms after stimulus presentation to estimate the response r to each stimulus s. The number of spikes counted on each trial varied between 5 and 30 spikes depending on the neuron. To precisely quantify information transmission given our experimental constrains (e.g., number of trials), it was necessary to reduce the number of possible neural responses. We therefore divided firing rates in five classes ensuring an adequate sampling of these values ($r \in R = \{1, 2, 3, 4, 5\}$) (Panzeri et al. 2007). The stimuli were separated into two classes since we were interested in obtaining information about two adjacent morph levels ($s \in S = \{1, 2\}$). Therefore, responses to faces of the same morph level were pooled into one single category (0%, 20%, 40%, etc.). Each condition contained the exact same number of trials, and, therefore, information bit rates could be used to compare the conditions, although they were not corrected for low sample numbers. We considered the category boundary to be the point along the continuum with maximal sensitivity or, in this case, with the highest information transmission. To precisely estimate this point, we fitted Gaussian curves to the mean mutual information values, since those values showed a clear inverted U shape. To calculate confidence intervals, we used bootstrapping statistics. On each iteration (repeated 100 times), we randomly sampled 70% of the face-selective neurons, recalculated mean values, fitted a Gaussian curve, and estimated the categorical boundary given by the peak of the Gaussian curve. We computed a null hypothesis distribution of boundaries by recalculating information values using shuffled labels, repeating the subsampling procedure, and fitting Gaussian curves (100 iterations). The mean boundary in the case of the shuffled bootstraps was at 50% (±1.5 SE) and significantly different compared with the mean boundary calculated directly from the data ($P < 10^{-4}$ in both monkeys by a Wilcoxon signed-rank test).

Monkey preferential looking experiment. After the recordings concluded, the same two monkeys participated in this experiment. Each trial was initiated after the monkey fixated within a square region of $10 \times 10°$ located at the center of the screen, which was indicated by a fixation cross. Within this region, a face (of $\sim 10 \times 10°$ in size) was presented as long as the monkeys looked at it, but for no longer than 5 s. If the monkey fixated out of the region containing the face, or after 5 s of face inspection, the face was replaced by a fixation cross. When the monkey gazed again at the fixation cross within the $10 \times 10°$ square region, a blank stimulus (a gray square of size $10 \times 10°$) was presented. As for the face, the blank stimulus was presented as long as the monkeys looked at it or at most during 5 s. The faces and blanks were alternated in this way until both together were viewed for a total of 20 s. Face stimuli were videos made by moving a virtual camera around full-color mode 3-D faces (from −20 to 20° along the faces' vertical axis). One of three types of faces was randomly presented on each trial: 100% monkey, 50% monkey, or 0% monkey, all taken from only one morph trajectory. At the end of every trial, during the period of 5 s before the next trial started, the monkey was provided with juice.

Human tasks. For the "same/different task," 10 subjects attended to a face shown for 500 ms followed by a 1-s blank period and also by a second face presented for 500 ms. As in the electrophysiology experiments with monkeys, faces were presented at random viewing angles (−20 to +20°) and sizes (8–12°). On "same" trials, two different views of the same face were presented at each morph level from 10% to 90%. On "different" trials, two faces from the same morph trajectory but differing by 20% in their morph level (+10% and −10% from the morph center) were presented. Subjects had to indicate whether the face was the same or different and received feedback about their performance after each trial. In a second experiment, the same subjects had to explicitly categorize face images with morph levels ranging from 0% to 100% with increments of 10%. The same images were presented during 500 ms followed by a blank period of 1 s in which subjects had to press a button to indicate the category of the image (human or monkey). Trials ended with a blank period of 1 s. In both experiments, subjects were instructed to fixate at a cross, which was placed at the center of the screen during the whole trial. Additionally, we instructed them to avoid concentrating their attention on a particular feature or subspace of the images but rather to respond "intuitively" (without thinking about it) based on their general impression. Subjects could give two different responses by pressing one of the two buttons reachable with the left and right hands, respectively. At the beginning of the experiment, subjects were instructed to press one of the buttons to choose one of the two options (same or different in *experiment 1* and human or monkey in *experiment 2*). To select one of the two types of responses, half of the subjects used the left hand, whereas the other half used the right hand. This was done to avoid any artifacts caused by pairing one hand to a particular response.

RESULTS

We used realistic 3-D morphed face stimuli that spanned the continuum between human and monkey faces, as shown in Fig. 1*A*. In contrast to the majority of previously published work using face stimuli, we presented faces to observers rendered from 3-D face models at random orientations (±20°) on each trial, discouraging observers from attending to specific spatial features. Examples of those face images are shown in Fig. 1*B*. To generate linear morphs, we used a state of the art method based on machine learning (Steinke et al. 2005). This method establishes a correspondence between surface points on each of the faces in 3-D using a SVM algorithm. Once this correspondence is known, one face can be transformed into another by linearly moving all corresponding points. This ensures that faces are morphed on a strictly linear trajectory. To verify that the morphs were actually linear in terms of physical characteristics, we performed detailed simulations using image statistics and a Gabor filter bank model (see Supplemental Material). We show that face pairs differing by a constant amount in the morph space were equally similar in terms of physical attributes, regardless of the position along the morph continuum. This confirms that in terms of physical characteristics, the monkey-human face morphs were indeed linear. We used these morphed face stimuli to study activity from single neurons in the monkey IT cortex and to gather psychophysical evidence about the face species boundary in both monkey and human observers. Morphed faces resulted from the linear interpolation of two monkey and two human faces, leading to four morph lines (see Fig. 1*A*). Since we focused on species effects here, stimuli were grouped according to their morph level, irrespective of the morph line. For the neural recordings, we included six objects (fruits, furniture, etc.) in our stimulus set to identify face-selective cells, which are neurons that discriminate between faces and objects (Supplemental Fig. S1 shows more examples of the images used).

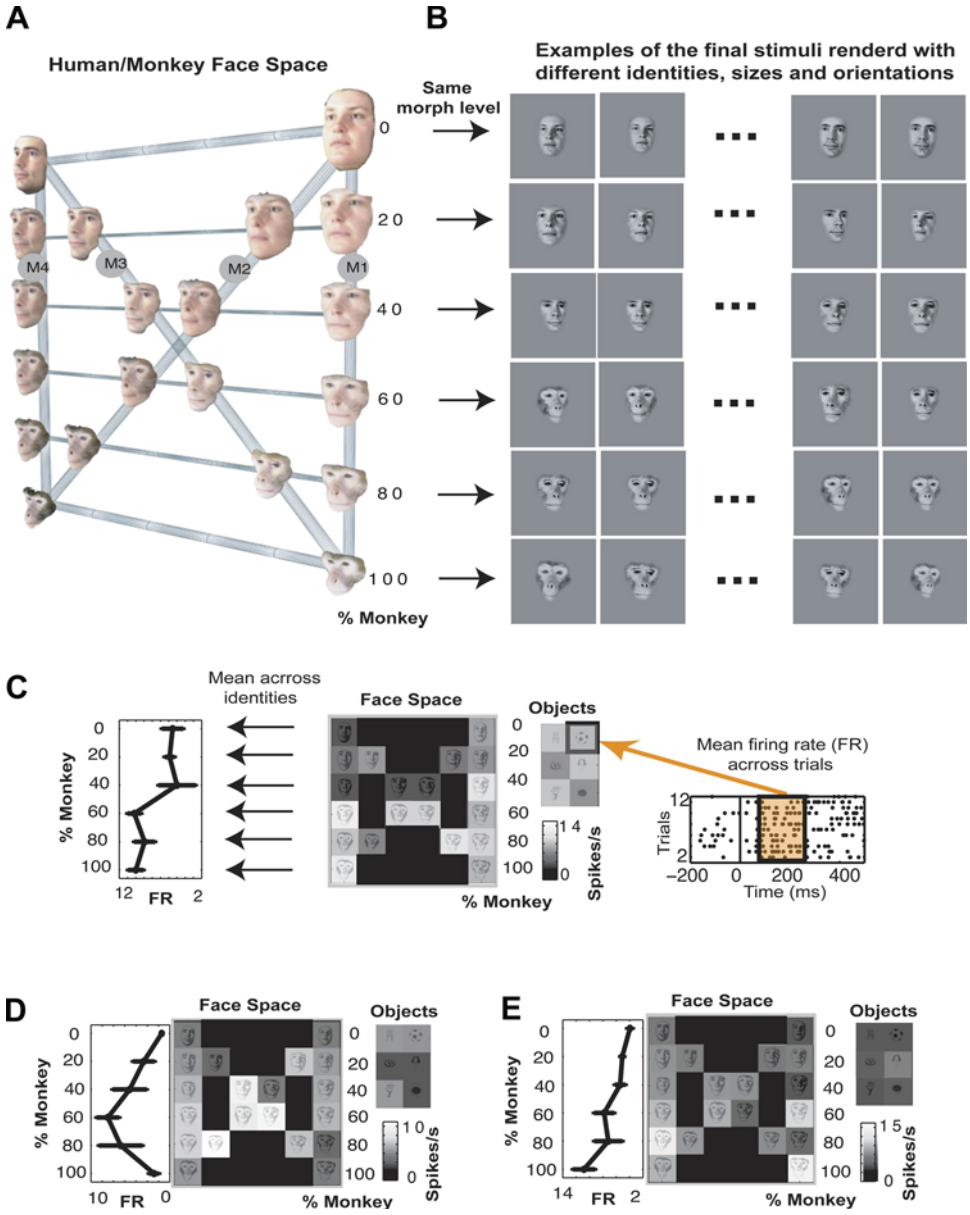

Fig. 1. Human/monkey face space and responses of exemplar single units. *A*: the face space was composed by four morph trajectories (M1–M4) that resulted after morphing two human into two monkey faces (shown at the corners of the space) in five steps (20% change). The horizontal axis of the space reflects differences in identity, whereas the vertical axis represents changes in the "species level." Morphs are arranged in descending order going from humans (0%) to monkeys (100%). *B*: from the three-dimensional face space, we rendered images of faces with different identities (taken from different morph trajectories), orientations, and sizes. All images were grayscale with normalized contrast and luminance values. *C–E*: neural responses of three exemplar units with "step-like" (*C*), "inverted U-shaped" (*D*), and "monotonic-like" (*E*) tuning curves. The gray layer superimposed on each stimulus illustrates the strength of the response. Face stimuli are arranged as in *A*; objects are placed on the *right*. As shown by the raster plot on the *right* part of *C*, the gray color code accounts for the average number of spikes recorded 100–300 ms after stimulus presentation. For each neuron, the range of the response (in spikes/s) is indicated by the color bar on the *bottom right*. Curves on the *left* are the mean firing rates (FRs) across all faces of the same morph level. The neuron in *C* was responsive to faces and objects, whereas neurons in *D* and *E* were only responsive to faces.

Single neuron activity changes systematically along the monkey-human continuum. We recorded the activity of 408 single units (194 single units in *monkey M1* and 214 single units in *monkey M2*) in area TE of the IT cortex during a fixation task. As shown in Fig. 2, *A* and *B*, recordings were performed below the superior temporal sulcus and distributed along 6 mm of the AP axis (relative to the interaural line). Mean responses across all recorded cells showed no consistent differences in both monkeys between the responses to monkey and human faces (mean firing rates: *monkey M1*, 7.88 and 7.69 spikes/s for human and monkey faces, respectively, $P > 0.1$ by paired *t*-test; *monkey M2*, 6.93 and 7.13 spikes/s, $P < 0.05$ by paired *t*-test). We found, however, that the activity of many neurons was systematically modulated by the morph level. We distinguished three major classes of neurons, examples of which are shown in Fig. 1, *C–E*, and Supplemental Fig. S3. Step-like neurons, which show a sharp change in activity at an intermediate morph level, have been previously associated with categorical perception, because they tend to show more similar activity to stimuli within categories than between categories (Freedman et al. 2001 and 2003; Akrami et al. 2009). Monotonic-like neurons may reflect changes in the physical properties of the face stimuli, with a general preference for either human or monkey faces. The class of inverted U-shaped tuned neurons is of particular interest, because such neurons tend to be more active at intermediate morph levels near the category boundary. From all cells significantly correlated to any of the three functions (49 of 194 neurons or 25% in *monkey M1* and 30 of 214 neurons or 14% in *monkey M2*), step-like neurons were encountered less frequently (7 of 49 neurons or 14% in *monkey M1* and 7 of 30 neurons or 23% in *monkey M2*). More common in the population were neurons showing monotonic-like (25 of 49 neurons or 51% in *monkey M1* and 10 of 30 neurons or 33% in *monkey M2*) or inverted U-shaped (17 of 49 neurons or 35% in *monkey M1* and 13 of 30 neurons or 43% in *monkey M2*) morph level tuning. A few neurons significantly correlated with both monotonic-like and step-like functions (11 of 194 neurons or 6% in *monkey M1* and 3% in *monkey M2*). In such

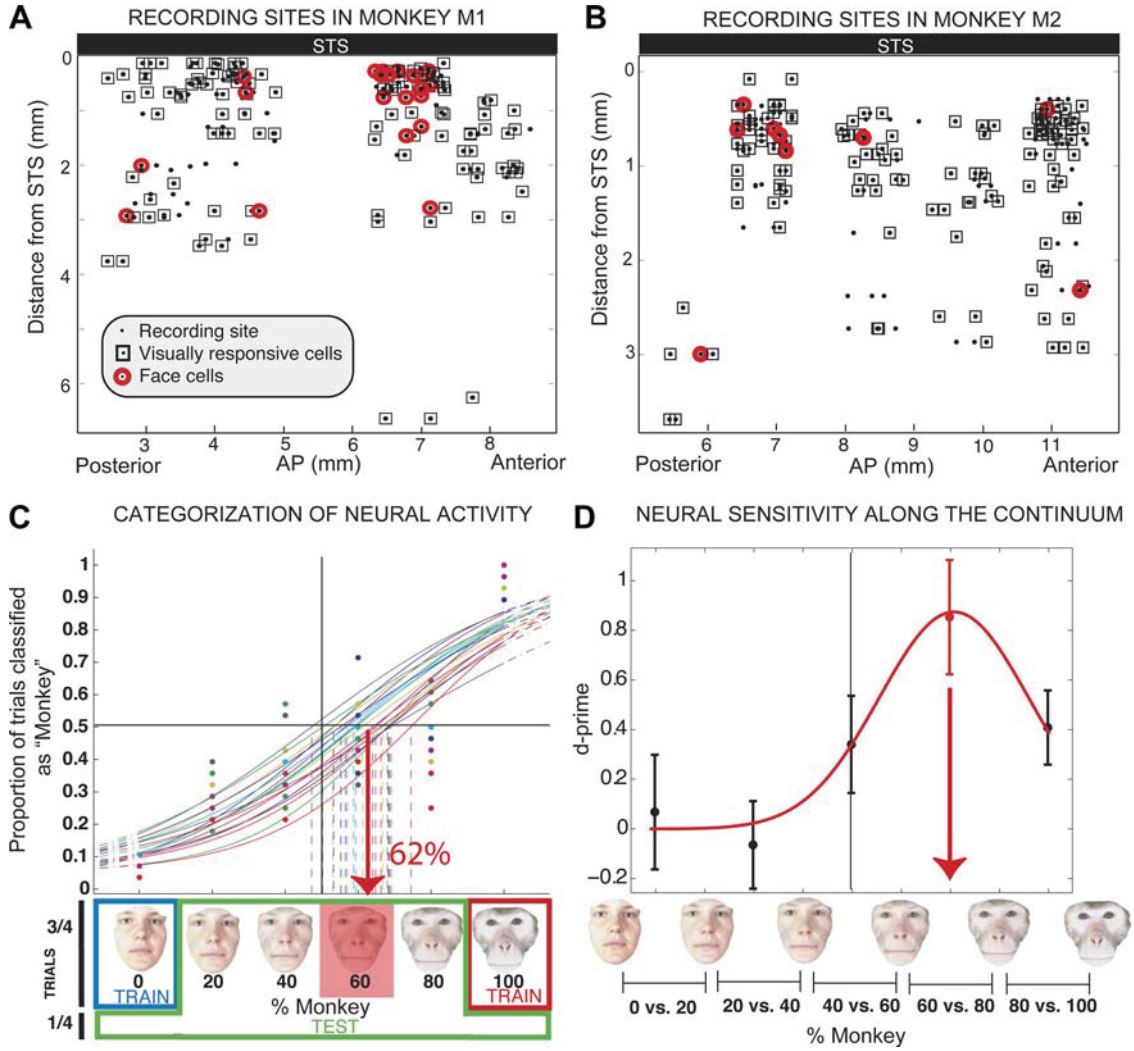

Fig. 2. Recording sites and population analysis using the pattern classifier. *A* and *B*: recording sites in *monkeys M1* and *M2*. The *x*- and *y*-axes indicate the distance (in mm) to the interaural line in the anterior-posterior (AP) axis and to the superior temporal sulcus (STS), respectively. Recording locations are marked by solid circles. Sites in which visually responsive and face-selective cells were encountered are marked by solid squares and red circles, respectively. *C* and *D*: estimation of the category boundary using whole neural population activity and the pattern classifier. *C*: the horizontal axis represents the continuum from human (0%) to monkey (100%) illustrated with faces of the M1 morph trajectory for clarification (see Fig. 1*A*). The vertical axis indicates the proportion of test trials labeled by the classifier as "monkey." Training data were exclusively chosen from a subset (3/4 of the trials) of responses to human (0%) and monkey (100%) faces (enclosed in blue and red boxes along the *x*-axis, respectively). In the test phase, the classifier labeled the remaining responses (1/4 of the trials) to human and monkey faces as well as all trials with responses to the morphed faces (enclosed in a green box along the *x*-axis). To obtain confidence intervals, we iterated 100 times randomly selecting 75% of the total number of neurons. The colored circles, curves, and dashed lines represent the classifier's responses, psychometric functions, and category boundaries calculated on every single iteration, respectively (only 20 iterations are shown for simplicity). The mean category boundary (62%, marked with the red arrow) was significantly shifted away from the center of the continuum toward the monkey side ($P < 0.05$ by a Wilcoxon signed-rank test vs. "shuffled bootstraps"). *D*: classifier performance in the discrimination of neural responses to adjacent pairs of morphed faces. Performance (d') is shown in the vertical axis as a function of the pair of responses compared and illustrated in the horizontal axis by the five pairs of faces (0% vs. 20%, 20% vs. 40%, 40% vs. 60%, etc). Performance reached a peak in the 60% versus 80% comparison, which was significantly greater than shuffled bootstraps ($P < 0.05$), the mean across the other pairs ($P < 0.05$ by a Wilcoxon signed-rank test), and the mirror case on the other side of the continuum (20% vs. 40%, $P < 0.01$ by a Wilcoxon signed-rank test).

cases, the labels of the cells were assigned according to the greatest correlation value. The remaining neurons (145 of 194 neurons or 75% in *monkey M1* and 184 of 214 neurons or 86% in *monkey M2*) were unresponsive (26 of 194 neurons or 13% in *monkey M1* and 71 of 214 neurons or 33% in *monkey M2*) or did not significantly correlated with the defined tuning functions (119 of 194 neurons or 61% in *monkey M1* and 113 of 214 neurons or 53% in *monkey M2*).

Decoding the monkey-human category boundary from the neural population reveals a shift toward own species. We applied a machine learning algorithm to determine the location of the category boundary in the species continuum between human and monkey faces considering all recorded cells. The logic of this approach was to train a classification algorithm to distinguish between the pattern of neural activity elicited by human and monkey faces and then let it classify the neural responses to the morphed faces along the monkey-human continuum as belonging to one of the two categories (human or monkey). We trained the classifier with a random subset (75%) of trials in which the responses to human (0% morph level) and monkey (100% morph level) faces were learned by the classifier. The classifier was then tested with the remaining (25%) trials containing the neural responses to faces at 0% and 100% morph level as well as all the trials with the responses to faces

at intermediate morph levels, ensuring a separation of test and training data. The procedure was repeated 100 times using also new randomly selected neurons (75% of the total population) to obtain confidence intervals. At each iteration, a psychometric function was fitted to the classifier decisions, and the category boundary was estimated (Fig. 2*C*, colored curves and vertical dashed lines). We applied this method to the entire population of recorded IT neurons, thus precluding any selection biases. As shown in Fig. 2*C*, the classifier determined the boundary between the human and monkey species to be at a morph level of 62% in the pooled data of the two monkeys, but also consistently in each monkey separately (64% and 61% in *monkeys M1* and *M2*, respectively). The boundary was significantly shifted away from the center of the human to monkey continuum at the 50% morph level, toward the side of the monkey faces (Wilcoxon signed-rank test vs. shuffled bootstraps, $P < 0.01$ for both monkeys and $P < 0.05$ on single monkey data; see METHODS for details). This boundary shift suggests the existence of a bias in the face representation towards own-species faces in the monkey cortex.

To further study the boundary shift, we examined whether faces within a category were indeed discriminated more poorly than faces between categories separated from each other by an equal physical amount. A peak in the discrimination performance is indicative of a sharp transition within the morph continuum, whereas the lack of such a peak suggests a smooth representation of the morph continuum with no measurable transitions. We thus submitted to the same classifier described above neural responses to adjacent pairs of morphed faces along the continuum (morph levels: 0% vs. 20%, 20% vs. 40%, 40% vs. 60%, 60% vs. 80%, and 80% vs. 100%). For each pair of morphed faces, the classifier estimated how different the corresponding neural activation patterns were. For each comparison, the classifier was trained with a randomly selected subset (75% of trials) of the neural data of the given two classes. Classifier performance was estimated by examining the assignment of the remaining responses (25% of trials) to the correct class. This procedure was repeated 100 times with new randomly selected neurons (75% of the total) to obtain confidence intervals. Classifier performance is related to the degree of similarity between the neural activation patterns elicited by the two classes: low performance indicates similar activation patterns, whereas high performance indicates substantial differences in activation patterns. As shown in Fig. 2*D*, we found a peak in classifier performance for the 60% versus 80% morph level classification when the data of both monkeys (mean $d' = 0.85$) were pooled, but also consistently in both monkeys separately (mean d' in *monkey M1*: 0.65 and *monkey M2*: 0.71). In this comparison, performance was significantly higher than shuffled bootstraps ($P < 0.05$ in both monkeys) and significantly greater than the mean performance across the other pairs ($P < 0.05$ in both monkeys by a Wilcoxon signed-rank test). This procedure follows that used in other studies regarding categorical perception of facial attributes. In addition, the classifier performance was greatly enhanced ($P < 0.01$ for both monkeys together and $P < 0.05$ in single monkey data by a Wilcoxon signed-rank test) compared with the mirror condition on the other side of the morph space center (20% vs. 40% morph level). Taken together, the boundary shift estimated using the population classifier and the corresponding peak in discrimination performance represent strong evidence for an own-species bias in the categorical representation of faces in the macaque IT cortex.

Shifted category boundary estimated from single face-selective neurons. While the above analysis used machine learning to classify neural activity of the entire population of neurons, we went on to demonstrate that face-selective single neurons also provide strong support for an own-species bias in the categorical representation of species. For this analysis, we selected "face neurons," which responded more to faces than to object stimuli, in each monkey according to standard criteria (see METHODS). Note that these neurons tended to be anatomically distributed throughout the recording regions (see Fig. 2, *A* and *B*), although there was some apparent clustering near AP 6 in both monkeys, a region that has been termed the "middle face patch" using fMRI. We did not encounter areas where only face neurons were located in our recordings. In addition, face neurons were also found to be distributed across the remaining recording sites. We did not observe consistent effects of face species on mean responses across these cells (mean firing rate in *monkey M1* of 9.96 and 8.94 spikes/s for human and monkey faces, respectively, $P > 0.1$ by paired *t*-test; mean firing rate in *monkey M2* of 7.27 and 7.85 spikes/s, $P > 0.5$ by paired *t*-test). For the face-selective neurons, we used information theory (Panzeri et al. 2007) to verify the existence and determine the location of the category boundary. We computed how much information each neuron communicated about pairs of faces separated by a constant physical distance (20% morph level) at each point along the monkey to human continuum. We averaged the mutual information values at each morph pair across neurons. Since the resulting curves displayed clear peaks around the center of the continuum (inverted U shaped), we fitted Gaussian functions to these data to precisely estimate the location of the boundary, as indicated by the position of maximal sensitivity. As the red curves shown in Fig. 3, *A* and *B*, demonstrate, the peak of the average information was significantly shifted toward the monkey side (*monkey M1*: 68% morph level and *monkey M2*: 56% morph level, confidence intervals were obtained using bootstrapping, $P < 10^{-4}$ in both monkeys by a Wilcoxon signed-rank test vs. shuffle bootstraps; see METHODS for details). This provides confirmation of the own-species face representation bias and demonstrates that this effect is present in face cells. Interestingly, the population of face neurons was composed not only of step-like neurons but also contained equal or greater numbers belonging to the other classes of monotonic-like and inverted U-shaped neurons. Additionally, we computed the same mutual information analysis using the least face-selective neurons [according to a standard face selectivity index (Tsao et al. 2006) and considering the same number of face-selective cells to avoid any bias]. We found that, in both monkeys, the mean categorical boundary was placed at the center and was not significantly different from the null hypothesis (shuffled bootstraps) distribution ($P > 0.1$ in both monkeys by a Wilcoxon signed-rank test). This suggests that category information is not confined to neurons with a particular tuning curve along the monkey human continuum but rather is distributed among the population with a prominent influence in the face-selective cells.

Psychophysical evidence for an own-species bias in the categorical perception of face species in human and monkey observers. Together, these findings indicate an own-species bias in monkey IT cortical face representation, as revealed by a shifted category boundary toward the monkey side of the species continuum. We further asked whether these neural

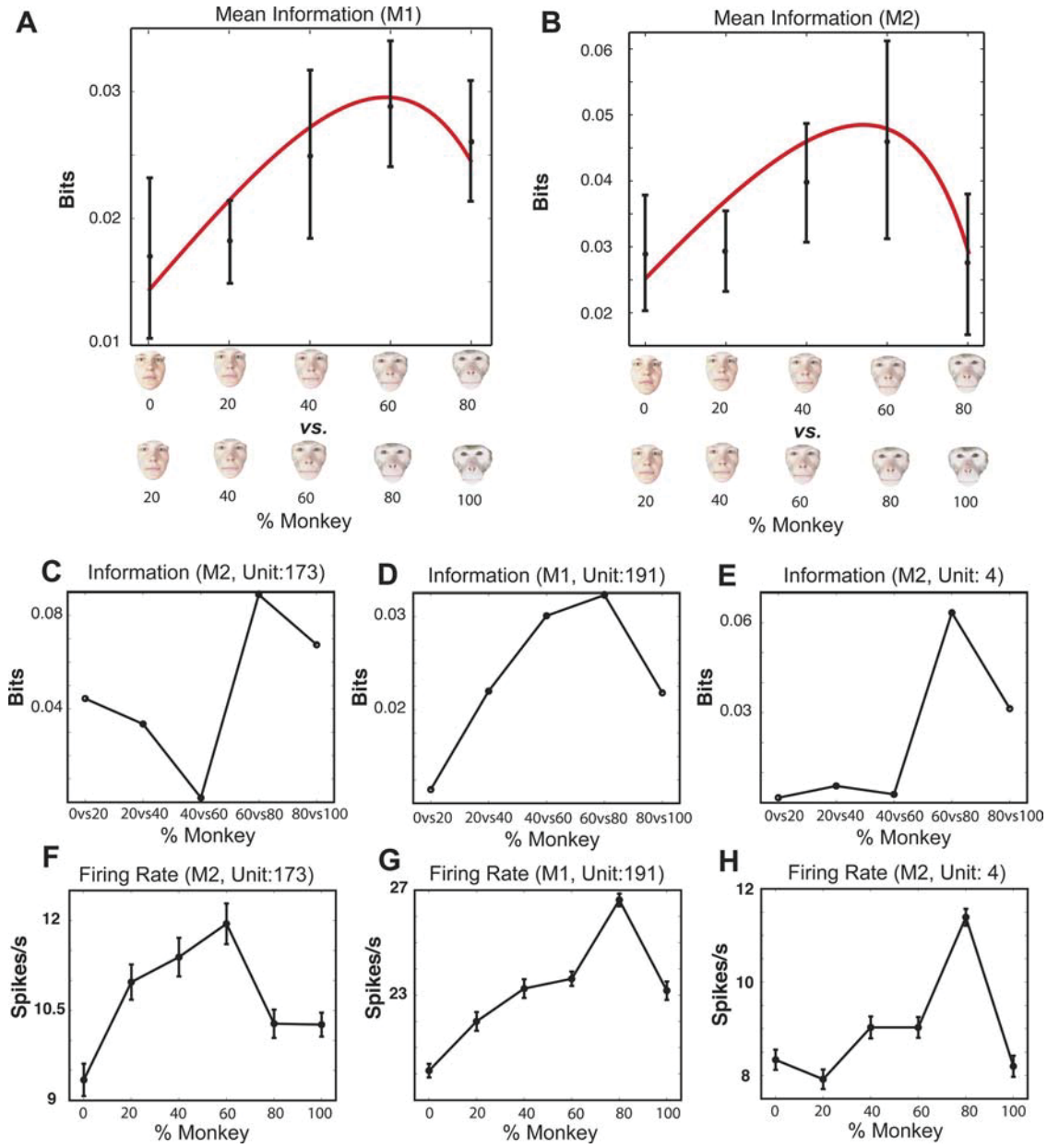

Fig. 3. Discriminability of face-selective neurons along the morph continuum. *A* and *B*: discriminability in "face-selective" cells was evaluated in terms of the information (bits in the vertical axis) transmitted about different pairs of stimuli (0% vs. 20%, 20% vs. 40%, 40% vs. 60%, etc., represented on the horizontal axis). As indicated by the red curves fitted to the mean information values (solid circles), the peak in the sensitivity was shifted from the center to the side of the monkey prototype (~68% and 66% in *monkeys M1* and *M2*, respectively, mean and confidence intervals obtained using bootstrapping, $P < 10^{-4}$ in both monkeys by a Wilcoxon signed-rank test vs. shuffled bootstraps; see METHODS for details). *C–E*: three examples of face cells (*unit 191* in *monkey M1* and *units 173* and *4* in *monkey M2*) showing clear peaks in their information transmission when responses to morphed faces at 60% and 80% of the continuum were compared. However, when their FRs along the continuum were assessed (*F–H*), it was possible to observe different tuning curves rather than a predominant type of tuning. From these exemplar cells, two cells (*F* and *G*) were categorized as inverted U shaped and monotonic like, respectively. The third cell (*H*) did not fall into any of the categories.

effects also influenced the behavior of the monkey. We used a preferential-looking paradigm (Dahl et al. 2007; Ghazanfar and Logothetis 2003; Humphrey 1974), which relies on the observation that novel or out-of-context items tend to attract gaze and are scrutinized longer. We thus presented stimuli corresponding to human, monkey, and 50% morphed faces for 20-s periods and determined the fraction of time that the monkeys gazed at each of these stimulus types. Since monkeys spend most of their time in conspecific groups, we expected that the looking time would be greater for human than monkey faces since human faces are more novel and out of context. We also predicted that a 50% morph stimulus should be treated like a human and not like a monkey face, given that the category boundary falls at 60% of the human-monkey continuum. As shown in Fig. 4, we found that for both monkeys the proportion of time viewing 50% morphed faces (mean *monkey M1*: 0.603 and *monkey M2*: 0.569) was statistically identical ($P > 0.1$ by paired *t*-tests) to the viewing proportions for human faces (mean *monkey M1*: 0.585 and *monkey M2*: 0.508) but statistically different ($P < 0.05$ by paired *t*-tests) from monkey face viewing proportions (mean *monkey M1*: 0.468 and *monkey M2*: 0.345). This pattern of results confirmed our predictions and

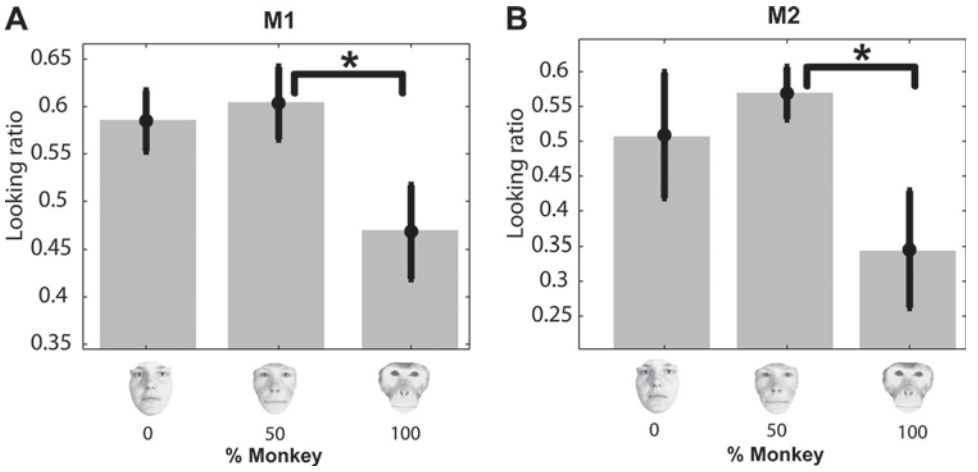

Fig. 4. Results of the behavioral experiments with monkey observers. *A* and *B*: preferential looking ratio obtained for *monkeys M1* (*A*) and *M2* (*B*) on each of the tree conditions (faces with 100%, 50%, and 0% monkey level). The vertical axis in each plot shows the mean looking ratio, which was calculated as the proportion of time within a trial in which the monkeys looked at faces compared with a blank image. Error bars represent SEs. In both monkeys separately, we found a statistically significant difference only between the comparison of 100% versus 50% monkey ($P < 0.05$ by paired *t*-test) but not in the comparison of 50% versus 0% monkey ($P > 0.1$).

provides independent behavioral evidence for a shift in the category boundary away from the center of the morph space and toward the monkey side.

In a final step, we asked whether categorical effects could also be seen in human observers using our morphed stimulus set. To this end, we conducted a psychophysical experiment to measure the performance of human subjects in distinguishing faces at constant physical distance (20% morph level) along the species continuum. As shown in Fig. 5*A*, the performance of the subjects in terms of d' showed a clear peak as a function of morph level. We fitted a Gaussian function to the average performance and estimated the location of the boundary to be at 33% morph level. To demonstrate a categorical perception of the continuum (Beale and Keil 1995; Calder 1996; Etcoff and Magee 1992; Levin and Angelone 2002; Levin and Beale 2000), we compared the mean sensitivity around the boundary (20% vs. 40% and 30% vs. 50) against the mean sensitivity across all other pairs ($P < 0.01$ by *t*-test). By comparing the sensitivity close to the previously estimated boundary (20% vs. 40% and 30% vs. 50%) and the sensitivity in the mirror side of the continuum (50% vs. 70% and 60% vs. 80%), we confirmed the significance of this bias toward human faces ($P < 0.0001$ by *t*-test). The category boundary shift for human subjects was toward the human side and thus in the opposite direction, but of similar magnitude, compared with that seen in the monkey results described above. This experiment provides an implicit measure of the human ability to distinguish faces along the species continuum. We complemented this with an explicit task where we asked human subjects to categorize briefly presented morphed faces as human or monkey. The results shown in Fig. 5*B* demonstrate that this explicit task yielded identical results compared with the implicit measure, with the category boundary estimated to be at 41% morph level [significantly shifted from 50%, $P < 0.01$ based on bootstrap simulations using the psignifit toolbox (version 2.5.6) for Matlab, which implements the maximum likelihood method (Wichmann and Hill 2001)].

Linearity of morph space confirmed by statistical properties of the face morph images. The method used to create the human/monkey morphs guarantees a linear interpolation of

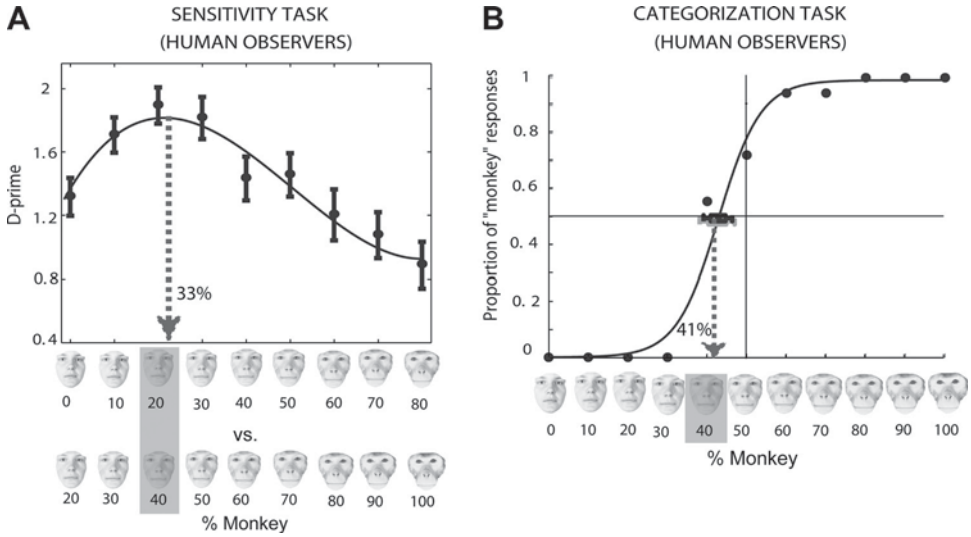

Fig. 5. Results of the psychophysical experiments with human observers. *A*: subjects' sensitivity to detect differences along the species continuum. The d' value (vertical axis) was plotted as a function of the position of the morph center in the species continuum (horizontal axis). To better estimate the position of the category boundary, we fitted a Gaussian curve and found the point in the species continuum where the curve reached its maximum. The category boundary was shifted from the center toward the human side (mean boundary: 33%). *B*: results of the human or monkey face classification experiment. The vertical axis shows the proportion of images perceived as monkeys as a function of their position along the species continuum, shown as the horizontal axis. To find the human/monkey perceptual boundary, we fitted a psychometric function and looked for the point at the human/monkey continuum that caused the responses to be at chance level (0.5). The category boundary in this case was placed at 41%, significantly shifted from the center toward the human side of the continuum ($P < 0.01$ based on bootstrap simulations).

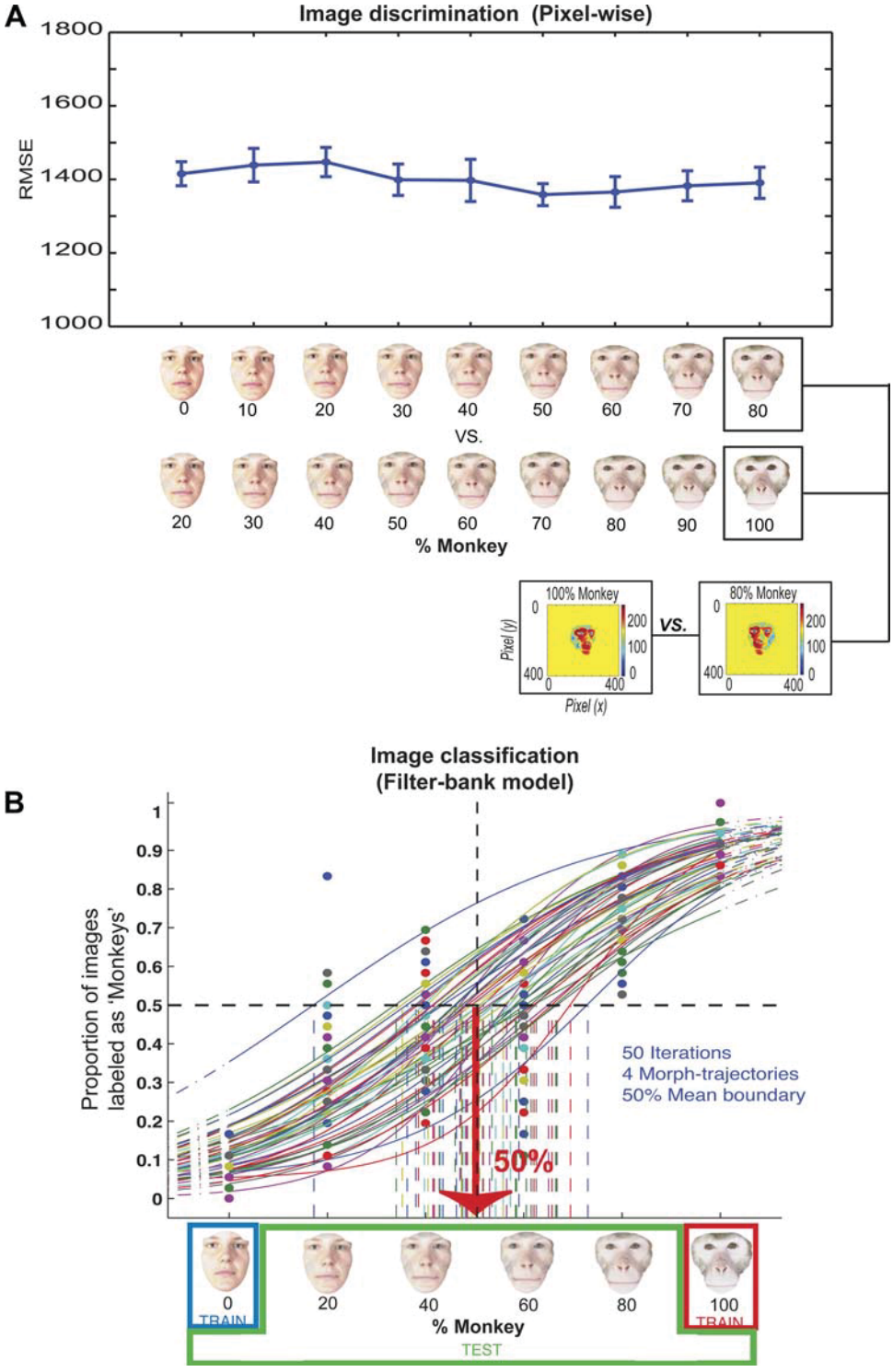

Fig. 6. Statistical properties of the images verify the linearity of the morph trajectories. *A*: the blue curve shows the average root mean square error (RMSE; vertical axis) and SEs for each comparison (horizontal axis). As in the psychophysical experiments, pairs of images compared were taken from the same morph trajectory but with different views and sizes. The two pictures below the plot show the pixel values of two exemplar images (100% and 80% monkey), represented as 400 × 400-pixel maps with values ranging from 1 to 256. *B*: classification performance of an "unbiased" classifier based on standard models of object recognition in the visual cortex (see the Supplemental Material for details). Performance is shown as the proportion of images (vertical axis) along the continuum (horizontal axis) classified as monkeys. To compute confidence intervals, the classification procedure was repeated 50 times by randomly selecting a subset of image features as well as train and test image sets (see the Supplemental Material for details). Colored circles and curves show the performance on single iterations in which the positions of the boundaries (vertical dashed lines) were calculated. As expected from a linear continuum, the average position of the boundary was not statistically different from 50% (51 ± 1.54%).

two 3-D surfaces (Steinke et al. 2005). Nevertheless, we decided to confirm this linearity using additional control analyses on the statistical properties of the images. Images were analyzed in two ways: *1*) a pixel-based comparison computing the root mean squared error (RMSE) between pairs of images and *2*) using an image classification model inspired by standard models of the hierarchical processing of information in the visual cortex (Riesenhuber and Poggio 1999; Serre et al. 2007).

The pixel-based analysis quantifies differences between pairs of images in terms of their global contrast and luminance levels. Since the simplicity of this analysis allows us to test many images, we compared all images that were also compared by human observers in our experiments. Pairs of images were compared pixelwise using the RMSE (see the Supplemental Material for details). Figure 6*A* shows the means and SEs of the RMSEs for each condition. As the plot shows, there was no systematic modulation along the continuum and, more

importantly, the tests used to demonstrate categorical representation (performance around the boundaries found in human or monkey observers higher than the mean across all other conditions) were not statistically significant ($P > 0.3$ by t-tests). This indicates that images from adjacent morph levels differ by a similar amount in terms of basic image properties. From this it follows that the morphs themselves do not contain any clear boundaries or discontinuities, consistent with their generation by linear interpolation.

The second analysis uses a biological inspired approach that mimics the hierarchical processing in early stages of the visual cortex to quantify differences between image sets. The architecture of the model is based on standard models of hierarchical processing in the visual cortex (Riesenhuber and Poggio 1999; Serre et al. 2007) and consists of three layers (see Supplemental Fig. S2 and the Supplemental Material for details). The first layer filters the images according to the responses of a bank of Gabor wavelets. The second layer selects the most informative features using a simple mechanism based on the variance of the filters' outputs across all images. The third layer classifies images encoded by the previous layer using a linear SVM. In this case, the model was used to "discriminate" and "classify" the same images used in the electrophysiological experiments. Accordingly, faces from different morph trajectories, with different sizes and views, were considered together based only on their morph levels. Confidence intervals were calculated using bootstrapping statistics, randomly selecting independent sets of train and test images (see the Supplemental Material for details). In the discrimination task, the classifier was trained to distinguish between adjacent sets of images along the continuum (20% difference). The results of these simulations showed that the mean sensitivity along the continuum was not categorical, according to the standard tests previously explained ($P > 0.1$). In the classification task, the classifier was trained to label morphed images along the continuum as human or monkey. Figure 6*B* shows results of the 50 iterations (represented by the different colored dots and curves) in which the model classified images along the continuum. The mean position of the categorical boundary was not significantly different from 50% (grand mean 51% $\pm$ 1.54 SE). These results, together with the result of the RMSE analysis, confirmed that the morph continuum is indeed linear and that the mean boundary computed using an "unbiased" classifier is centered at 50% of the continuum.

DISCUSSION

We observed an own-species bias in the categorical representation of faces in monkey and human observers. The category boundary was, for each group of observers, shifted toward their own species. This indicates that the two species perceive the exact same face morph continuum in a fundamentally different way. Recent evidence suggests that visual experience during infancy plays a prominent role in shaping the face-processing system in humans and is thus likely to underlie the boundary shift (Sangrigoli and De Schonen 2004; Sangrigoli et al. 2005). One particularly pertinent recent study has examined the role of visual experience with faces in infant macaque monkeys: when newborn monkeys are raised without any exposure to faces for a period of 6–24 mo and then exposed to either human or monkey faces for a 1-mo period, they develop a lasting preference for faces of this species (Sugita 2008). These findings suggest that the boundary shift we observed may thus reflect extended visual expertise for own-species faces during infancy. Boundary shifts may serve as sensitive indicators of the relative strength of encoding for two categories. These boundary shifts could be estimated using explicit or implicit behavioral tasks but also by applying pattern classifiers to neural data allowing the read out of experiences that are not consciously accessible. This approach could be very useful for studying concept learning in human infants or children, and, indeed, there is already some interesting work in this direction (Pollak and Kistler 2002).

Human subjects have been shown to perceive a number of facial attributes categorically, including race (Levin and Angelone 2002; Lun Zhao 2008). Perception of own- and other-race faces exhibits two interesting asymmetries that are commonly referred to as "other-race effects": while categorization is more efficient for other-race faces, own-race faces are identified and recognized more easily (Levin 1996 and 2000). A recent study (Ge 2009) has demonstrated a correlation between these two aspects of the other-race effect and argues that they may both result from a common mechanism. We suggest that the category boundary shift observed at the level of IT cortex population activity may be this common mechanism and can account for both types of other-race effects: the shift of the category boundary from the center of the morph space toward the own species leads to an increase in sensitivity for faces closer to the own species. The capacity of neurons to signal information about a set of stimuli depends on to what extent firing rates elicited by the stimulus feature of interest fall within the dynamic range of the neuron. Neurons tuned to a boundary at the center of the morph space are differentially activated by stimuli close to the species boundary, and their dynamic range is allocated far from the own-species face stimuli. A boundary shift toward the own species results in the dynamic range also shifting into the own species part of the species continuum, making the neural dynamic range available for signaling individual differences of own-species faces. This enhancement in encoding resources for own-species faces results in a greater capacity for individuation. Nevertheless, this occurs at the expense of optimized encoding for category membership. The opposite is true for the other-species category, leading to a reduced capacity for individuation but easier read out of category membership. Thus, a boundary shift in the race continuum might be the underlying cause of both improved individuation and compromised categorization performance for own-race faces.

Our experimental design allows us to take advantage of the face expertise that human and monkey observers have acquired during their life. This permits us to investigate the effects of visual learning on face representations, since monkeys and humans have characteristic histories of viewing faces of each species. The laboratory monkeys participating in our study were raised in large monkey colonies containing dozens of animals for the first months after birth and in the laboratory are housed in groups of typically four to six animals. They also have, by comparison, limited contact with humans, such as animal care staff and laboratory scientists. Thus, particularly during early infancy, they are in contact almost exclusively with members of their own species. Conversely, human subjects have had almost exclusive visual contact with members of

their own species for most of their life, yet are familiar with monkeys from visits to zoos or television. Given these substantial differences in exposure and ethological relevance, own- and other-species faces are thus good candidates for revealing species differences in cortical categorical representations. In contrast to our findings for species, adult experience of human subjects strongly affects their perception of faces of unfamiliar race (Webster et al. 2004). There are two factors that might account for this difference: *1*) our monkey experts continued to be exposed to many human faces in addition to the monkey faces, whereas the subjects in the Webster et al. (2004) study were exposed predominantly to other-race faces during learning; and *2*) visual features share more characteristics among human faces of two different races compared with human versus monkey faces. Both these effects may enable stronger plasticity for other-race face learning compared with other-species face learning, leading to a boundary shift for other-race faces but not for other-species faces.

Our study demonstrates separable representations of own-species faces from those of another primate species in the monkey IT cortex. The monkey IT cortex contains many neurons that respond selectively to faces (Desimone et al. 1984; Leopold et al. 2006; Perrett et al. 1982; Tsao et al. 2006). These face cells are thought to underlie the capacity to recognize faces and to decode from them a variety of signals about identity, sex, gaze direction, or emotion. Previous work has indicated that individual face cells often respond to both human and monkey faces (Tsao et al. 2006), and multi-dimensional scaling analyses have revealed separate response patterns corresponding to faces of different species (Kiani et al. 2007). Our results agree with these studies in that differences in human and monkey faces were not encoded in the magnitude of the mean neural responses (Tsao et al. 2006) but instead in the pattern of the combined population activity (Kiani et al. 2007). Our results confirm the existence of separable representations and extend these findings by demonstrating a bias in favor of the own species representation that is reflected in a boundary shift between the representations of the monkey and human face categories. In humans, we observed a boundary shift that was similar in magnitude but opposite in direction. This suggests that visual expertise in humans leads to changes in the neural representation of natural categories. In addition, the existence of a category boundary is indicative of categorical perception of face species in humans, consistent with previous results (Campbell et al. 1997). These findings are part of a large body of studies documenting that humans perceive a variety of face attributes, including sex, race, or emotions, categorically (Calder 1996; Campbell et al. 1997; Etcoff and Magee 1992; Harnad 1987). Categorical perception of faces occurs when the visual system treats a continuous set of face stimuli, such as a set of morphed stimuli that span the continuum between two prototypes, as belonging to two discrete categories separated by the category boundary. The hallmark of categorical perception is that pairs of faces in a continuum differing by a given physical amount should be discriminated more accurately when that difference straddles the category boundary (Harnad 1987).

Recent work on categorization conducted in parallel in humans and monkeys has emphasized the commonalities in the neural representations of natural categories across these two primate species (Kriegeskorte et al. 2008). In particular, classification trees estimated from single neuron data in monkeys and fMRI data in human subjects show similar branching structure. Our results focus on a particular aspect of these data and show that species-dependent differences do exist in the category representation. This is not inconsistent with a common code for primate categorization. However, it suggests that while common principles and learning mechanisms may be at work in both species, particular species-specific experiences with certain categories will be reflected in the structure of their categorical representations. Indeed, both primate species share similar experiences with many natural categories such as fruit or body parts. Thus, our findings suggest while the neural code for face representation is species specific, the representations themselves are established by the same organizing principles.

In our neural recordings, monkeys performed a fixation task rather than a task that required them to actively sort stimuli into categories. We used this approach because we wanted to obtain information about how experiences with same and other species faces during everyday experiences were reflected in their neural representation. We thus use the well-established approach of Tanaka and colleagues, which has provided a wealth of information about object representation (Kiani et al. 2005; Kobatake and Tanaka 1994; Tanaka 2003). We specifically wanted to avoid training monkeys on categorization tasks, because this might lead to changes in the category boundary or other aspects of the neural representation. Indeed, it has been shown that categorization training can dramatically and rapidly alter neural responses, particularly in the parietal cortex (Freedman and Assad 2006) but also in other brain areas. Such training would be likely to mask the effects of interest in the present study. Tasks involving active sorting of stimuli into categories (Freedman et al. 2001; Nieder et al. 2002) always involve rewarding certain behavioral responses. In our case, rewarding or omitting rewards to morphed faces would be problematic during such a task, because monkeys will always adapt their responses to maximize the reward. The behavioral boundary may thus reflect the strategy used by the monkey more than the internal representation of the stimuli. To avoid this confound, we chose a preferential looking paradigm to provide behavioral evidence for a shifted category boundary in monkeys. We show that monkeys treated a 50/50 morph like a human face and not like a monkey face, consistent with a category boundary that is shifted toward the monkey side away from the morph space center.

In our study, only few neurons grouped faces along the human-monkey continuum into the two categories in a simple step-like fashion. However, the population contained categorical information about the species that the faces belonged to. The signature of categorical perception was an enhancement in the difference of neural responses to pairs of faces that straddled the category boundary compared with face pairs that did not. This enhancement could be observed both for the population of face neurons and for the entire population of recorded neurons analyzed using a pattern classifier. An important implication of our findings is that categories are represented in the brain not just by step-like neurons but also by other neurons that modulate their activity as a function of morph level between the categories. Behavioral categorization has a step-like function, since stimuli on one side of the category boundary are classified as belonging to *category A* and those on the other side already to *category B*. For this reason, neural

investigations into categorization have initially focused on neurons also showing such step-like behavior and thus directly mirroring the behavioral findings (Akrami et al. 2009; Freedman et al. 2001 and 2003). Neurons showing other behaviors (particularly behaviors that appeared hard to reconcile with behavioral categorization functions, such as inverted U-shaped tuning) received little attention. Our study emphasizes that neurons with all types of tuning contribute to categorization, not just step-like neurons. In addition, inverted U-shaped neurons are particularly implicated in categorization, because they exhibit maximum range of activity (and therefore selectivity) in the center of the stimulus continuum between the categories, where the categorical boundary is placed. Theories of cognitive psychology posit that the enhancement of discriminability at the category boundary is central to categorization (Harnad 1987). Our findings suggest that this is also true for the neural network underlying categorization in the primate temporal lobe.

ACKNOWLEDGMENTS

The authors thank Kristina Nielsen and Alexander Koch for contributions in the early stages of the project. The authors also thank Heinrich H. Bülthoff, Christian Wallraven, and Martin Breidt for the support to create the stimuli. The authors finally thank Andy Calder, Leslie G. Ungerleider, Christoph Kayser, and David Freedman for helpful comments on the manuscript.

GRANTS

This work was supported by the Max Planck Society and by an European Science Foundation European Young Investigator Award award (to G. Rainer).

DISCLOSURES

No conflicts of interest, financial or otherwise, are declared by the author(s).

REFERENCES

Akrami A, Liu Y, Treves A, Jagadeesh B. Converging neuronal activity in inferior temporal cortex during the classification of morphed stimuli. *Cereb Cortex* 19: 760–776, 2009.

Baker CI, Behrmann M, Olson CR. Impact of learning on representation of parts and wholes in monkey inferotemporal cortex. *Nat Neurosci* 5: 1210–1216, 2002.

Beale JM, Keil FC. Categorical effects in the perception of faces. *Cognition* 57: 217–239, 1995.

Calder AJ, Young AW, Perrett DI, Etcoff NL, Rowland D. Categorical perception of morphed facial expressions. *Visual Cogn* 3: 81–117, 1996.

Campbell R, Pascalis O, Coleman M, Wallace SB, Benson PJ. Are faces of different species perceived categorically by human observers? *Proc Biol Sci* 264: 1429–1434, 1997.

Dahl CD, Logothetis NK, Hoffman KL. Individuation and holistic processing of faces in rhesus monkeys. *Proc Biol Sci* 274: 2069–2076, 2007.

Desimone R, Albright TD, Gross CG, Bruce C. Stimulus-selective properties of inferior temporal neurons in the macaque. *J Neurosci* 4: 2051–2062, 1984.

Etcoff NL, Magee JJ. Categorical perception of facial expressions. *Cognition* 44: 227–240, 1992.

Freedman DJ, Assad JA. Experience-dependent representation of visual categories in parietal cortex. *Nature* 443: 85–88, 2006.

Freedman DJ, Riesenhuber M, Poggio T, Miller EK. Categorical representation of visual stimuli in the primate prefrontal cortex. *Science* 291: 312–316, 2001.

Freedman DJ, Riesenhuber M, Poggio T, Miller EK. A comparison of primate prefrontal and inferior temporal cortices during visual categorization. *J Neurosci* 23: 5235–5246, 2003.

Ge LZH, Wang Z, Quinn PC, Pascalis O, Kelly D, Slater A, Tian J, Lee K. Two faces of the other-race effect: recognition and categorisation of Caucasian and Chinese faces. *Perception* 38: 1199–1210 2009.

Ghazanfar AA, Logothetis NK. Neuroperception: facial expression linked to monkey calls. *Nature* 423: 937–938, 2003.

Grill-Spector K, Knouf N, Kanwisher N. The fusiform face area subserves face perception, not generic within-category identification. *Nat Neurosci* 7: 555–562, 2004.

Harnad S. *Categorical Perception.* Cambridge: Cambridge Univ. Press, 1987.

Haxby JV, Gobbini MI, Furey ML, Ishai A, Schouten JL, Pietrini P. Distributed and overlapping representations of faces and objects in ventral temporal cortex. *Science* 293: 2425–2430, 2001.

Humphrey NK. Species and individuals in the perceptual world of monkeys. *Perception* 3: 105–114, 1974.

Kiani R, Esteky H, Mirpour K, Tanaka K. Object category structure in response patterns of neuronal population in monkey inferior temporal cortex. *J Neurophysiol* 97: 4296–4309, 2007.

Kiani R, Esteky H, Tanaka K. Differences in onset latency of macaque inferotemporal neural responses to primate and non-primate faces. *J Neurophysiol* 94: 1587–1596, 2005.

Kobatake E, Tanaka K. Neuronal selectivities to complex object features in the ventral visual pathway of the macaque cerebral cortex. *J Neurophysiol* 71: 856–867, 1994.

Kriegeskorte N, Mur M, Ruff DA, Kiani R, Bodurka J, Esteky H, Tanaka K, Bandettini PA. Matching categorical object representations in inferior temporal cortex of man and monkey. *Neuron* 60: 1126–1141, 2008.

Leopold DA, Bondar IV, Giese MA. Norm-based face encoding by single neurons in the monkey inferotemporal cortex. *Nature* 442: 572–575, 2006.

Levin DT. Classifying faces by race: the structure of face categories. *J Exp Psychol Learn Memory Cogn* 22: 1364–1382, 1996.

Levin DT. Race as a visual feature: using visual search and perceptual discrimination tasks to understand face categories and the cross-race recognition deficit. *J Exp Psychol Gen* 129: 559–574, 2000.

Levin DT, Angelone BL. Categorical perception of race. *Perception* 31: 567–578, 2002.

Levin DT, Beale JM. Categorical perception occurs in newly learned faces, other-race faces, and inverted faces. *Percept Psychophys* 62: 386–401, 2000.

Lun Zhao BS. Own- and other-race categorization of faces by race, gender, and age. *Psychon Bull Rev* 15: 1093–1099, 2008.

Nieder A, Freedman DJ, Miller EK. Representation of the quantity of visual items in the primate prefrontal cortex. *Science* 297: 1708–1711, 2002.

Panzeri S, Senatore R, Montemurro MA, Petersen RS. Correcting for the sampling bias problem in spike train information measures. *J Neurophysiol* 98: 1064–1072, 2007.

Perrett DI, Oram MW, Hietanen PJ, Benson JK. Issues of representation in object vision. In: *The Neuropsychology of High-Level Vision: Collated Tutorial Essays*, edited by Farah MJ, Ratcliff G. Hillsdale, NJ: Erlbaum, 1994, chapt. 2, p. 33–1064–62.

Perrett DI, Rolls ET, Caan W. Visual neurones responsive to faces in the monkey temporal cortex. *Exp Brain Res* 47: 329–342, 1982.

Perrett DI, Rolls ET, Caan W. Temporal lobe cells of the monkey with visual responses selective for faces. *Neurosci Lett* S3: S358, 1979.

Pollak SD, Kistler DJ. Early experience is associated with the development of categorical representations for facial expressions of emotion. *Proc Natl Acad Sci USA* 99: 9072–9076, 2002.

Quiroga RQ, Reddy L, Kreiman G, Koch C, Fried I. Invariant visual representation by single neurons in the human brain. *Nature* 435: 1102–1107, 2005.

Riesenhuber M, Poggio T. Hierarchical models of object recognition in cortex. *Nat Neurosci* 2: 1019–1025, 1999.

Sangrigoli S, De Schonen S. Recognition of own-race and other-race faces by three-month-old infants. *J Child Psychol Psychiatry* 45: 1219–1227, 2004.

Sangrigoli S, Pallier C, Argenti AM, Ventureyra VA, de Schonen S. Reversibility of the other-race effect in face recognition during childhood. *Psychol Sci* 16: 440–444, 2005.

Serre T, Oliva A, Poggio T. A feedforward architecture accounts for rapid categorization. *Proc Natl Acad Sci USA* 104: 6424–6429, 2007.

Sigala N, Logothetis NK. Visual categorization shapes feature selectivity in the primate temporal cortex. *Nature* 415: 318–320, 2002.

Steinke F, Schölkopf B, Blanz V. Support vector machines for 3D shape processing. *Comp Graphics Forum* 24: 285–294, 2005.
Sugase Y, Yamane S, Ueno S, Kawano K. Global and fine information coded by single neurons in the temporal visual cortex. *Nature* 400: 869–873, 1999.
Sugita Y. Face perception in monkeys reared with no exposure to faces. *Proc Natl Acad Sci USA* 105: 394–398, 2008.
Tanaka K. Columns for complex visual object features in the inferotemporal cortex: clustering of cells with similar but slightly different stimulus selectivities. *Cereb Cortex* 13: 90–99, 2003.
Tsao DY, Freiwald WA, Tootell RB, Livingstone MS. A cortical region consisting entirely of face-selective cells. *Science* 311: 670–674, 2006.
Tsao DY, Moeller S, Freiwald WA. Comparing face patch systems in macaques and humans. *Proc Natl Acad Sci USA* 105: 19514–19519, 2008.
Vogels R. Categorization of complex visual images by rhesus monkeys. Part 2: single-cell study. *Eur J Neurosci* 11: 1239–1255, 1999.
Webster MA, Kaping D, Mizokami Y, Duhamel P. Adaptation to natural facial categories. *Nature* 428: 557–561, 2004.
Wichmann FA, Hill NJ. The psychometric function: I. Fitting, sampling, and goodness of fit. *Percept Psychophys* 63: 1293–1313, 2001.